ELSEVIER

Applied Surface Science 197–198 (2002) 746–756

applied surface science

www.elsevier.com/locate/apsusc

Polymers designed for laser ablation-influence of photochemical properties

T. Lippert[a,*], J.T. Dickinson[b], M. Hauer[a], G. Kopitkovas[a], S.C. Langford[b], H. Masuhara[c], O. Nuyken[d], J. Robert[d], H. Salmio[a], T. Tada[c], K. Tomita[c], A. Wokaun[a]

[a]*Paul Scherrer Institut, 5232 Villigen PSI, Switzerland*
[b]*Washington State University, Pullman, WA 99164-2814, USA*
[c]*Osaka University, Suita, Osaka 565-0871, Japan*
[d]*Technische Universtät München, 85747 München, Germany*

Abstract

The ablation characteristics of various polymers were studied at low and high fluences. The polymers can be divided into three groups, i.e. polymers containing triazene and ester groups, the same polymers without the triazene group, and polyimide as reference polymer. At high fluences similar ablation parameters, i.e. etch rates and effective absorption coefficients, were obtained for all polymers. The main difference is the absence of carbon deposits for the designed polymers. At low fluences (at 308 nm) very pronounced differences are detected. The polymers containing the photochemically most active group (triazene) exhibit the lowest threshold of ablation (as low as 25 mJ cm^{-2}) and the highest etch rates (up to 3 μm/pulse), followed by the designed polyesters and then polyimide. The laser-induced decomposition of the designed polymers was studied by nanosecond-interferometry. Only the triazene-polymer reveals etching without any sign of surface swelling, which is observed for all other polymers. The etching of the triazene-polymer starts and ends with the laser pulse, clearly indicating photochemical etching. The triazene-polymer was also studied by time-of-flight mass spectrometry (TOF-MS). The intensities of the ablation fragments show pronounced differences between irradiation at the absorption band of the triazene group (308 nm) and irradiation at a shorter wavelength (248 nm).

Keywords: Ablation; Triazene-polymer; TOF-MS; Interferometry

1. Introduction

Since the first report about removal of materials by lasers in the mid sixties [1] various new applications for lasers have been developed. Nowadays, laser ablation is used e.g. in medicine [2], art conservation [3], and thin film deposition [4]. Laser ablation of polymers was first reported in 1982 [5,6] and compared to conventional photolithography, but has unfortunately several disadvantages, i.e., low sensitivity [7], carbonization upon irradiation [8], and debris contaminating the surface [9] and optics. These problems are mainly the result of the application of standard polymers. Soon after the first reports about laser ablation of polymers the discussions about the ablation mechanism started. The suggested mechanisms range from thermal, over photothermal to photochemical [10–12]. In recent publications photothermal mechanisms are

* Corresponding author. Tel.: +41-56-310-4076; fax: +41-56-310-2485.
E-mail address: thomas.lippert@psi.ch (T. Lippert).

0169-4332/02/$ – see front matter
PII: S0169-4332(02)00404-X

favored [13] and photochemical contributions are treated as doubtful. Novel photopolymers were developed [14–18] to analyze whether there might be a photochemical contribution in laser ablation and to test whether it is possible to overcome some of the limitations of polymer ablation. Photochemical considerations have been applied for the design of these polymers. They were designed for an irradiation wavelength of 308 nm, because not all photolithographic processes require a resolution in the sub-micrometer range, and it is possible to de-couple the absorption of the photochemically active groups from the absorption of other parts of the polymer structure. This concept can be used to test whether the incorporation of photochemically active groups into the polymer chain improves the ablation characteristics. The most promising approach for the design of these 'laser ablation polymers' is the incorporation of the photochemically active chromophore into the polymer main chain. In this way, the polymer is highly absorbing at the irradiation wavelength and decomposes exothermally at well-defined positions of the polymer chain into gaseous products [19,20]. The gaseous products act as driving gas of ablation and carry away larger fragments, which could otherwise contaminate the surface. The polymers are therefore ablated without major modifications of the residual polymer surface, thus allowing a reproducible ablation [21].

From the standpoint of ablation properties, triazene group (–N=N–N<) containing polymers have been identified as the most promising candidates. Unfortunately problems are encountered with their stability with respect to the subsequent steps during a complete processing cycle, e.g. oxidation of the substrate [22].

Selected polyesters (PE) and polyestercarbonates (PEC) have also been found to exhibit good ablation

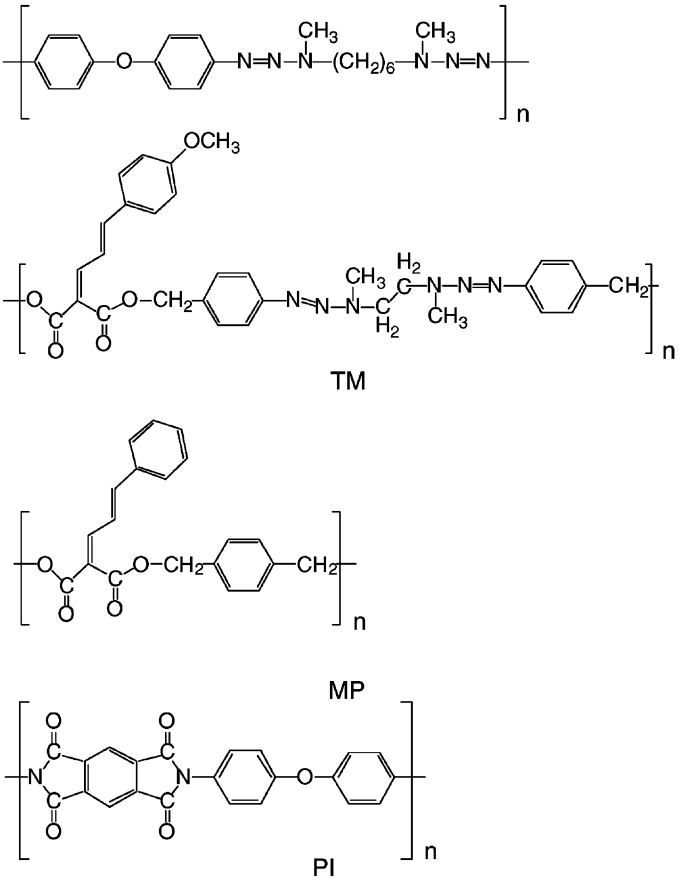

Scheme 1. Chemical structure of the polymers.

behavior [23]. The sensitivities of the PEs and PECs are lower as compared to the triazene-based polymers, but they exhibit a higher chemical stability. These polymers also produce small gaseous products (CO_2, CO) upon decomposition. The lower sensitivity of these PEs is most probably due to the quite low absorption coefficients at the irradiation wavelengths (<10 000 cm^{-1}). Therefore other PEs were developed which exhibit absorption coefficients similar to the triazene-polymers. It was also possible to create a mixed polymer which contains both (ester and triazene) groups in the polymer chain. To prove the concept of designing polymers for laser ablation, a reference polymer (polyimide, Kapton) with a similar absorption coefficient was included in this study. All of these polymers[1] (structures shown in Scheme 1), including PI, have similar absorption coefficients ($\approx 97\,000 \pm 5000$ cm^{-1}). The polymer that revealed the highest etch rate (lowest threshold) and the reference polymer were selected for additional studies at low fluences. Low fluences are most interesting for studying the ablation mechanisms, because additional processes during ablation, such as plasmas and inverse Bremsstrahlung, are only pronounced at higher fluences. The selected polymers were studied in more detail with additional analytical techniques (time-of-flight mass spectrometry (TOF-MS) and nanosecond-interferometry), other irradiation sources (excimer-lamps) and at different irradiation wavelengths.

2. Experimental

The polymers (TP, MP, and TM, shown in Scheme 1) were synthesized using standard polycondensation reactions. The syntheses are described in detail elsewhere [24,25]. For the reference polymer thin sheets (125 μm, Kapton® from Goodfellow) were used. A XeCl excimer laser (Lambda Physik, Compex 205; $\lambda = 308$ nm, $\tau = 20$ ns), was used as irradiation source for most experiments, with the exception of the interference experiments (see below) and the additional ablation studies at different wavelengths. For these studies an ArF excimer laser (Lambda Physik, LPX300; $\lambda = 193$ nm, $\tau = 20$ ns) and a frequency quadrupled Nd:YAG (Quantel Brilliant B, $\lambda = 266$ nm) laser were applied. The polymer films (50 μm thick) for the laser ablation experiments were prepared by solvent casting with THF or chlorobenzene as solvent. The procedure for determining the etch rates has been described in detail elsewhere [26]. The ablation experiments were performed at low (10–400 mJ cm^{-2}) and high fluences (up to 20 J cm^{-2}) to investigate the ablation behavior. In the case of 266 nm irradiation, the data analysis is more complicated, because the intensity beam profile is more complex (between Gaussian and Super-Gaussian), resulting probably in larger deviations in the data. The fluence for a defined part of the ablation crater was determined by fitting the intensity profile to the Gaussian/Super-Gaussian beam profile. This quite complicated routine may result in larger errors as compared to the analysis of data for the rectangular intensity profile of an excimer laser.

Excimer-lamps were used as an alternative source of excitation. The incoherent excimer radiation from a dielectric barrier discharge (silent discharge), operating in pure xenon, gas mixtures of krypton/chlorine and xenon/chlorine, provides intense narrow band radiation at $\lambda = 172$ nm (Xe_2^*), 222 nm ($KrCl^*$) and 308 nm ($XeCl^*$), respectively. More details about the excimer UV sources can be found in the literature [27,28]. The irradiance of the 308 nm lamp was determined by chemical actinometry [29] and is $\approx$25 mW cm^{-2}.

The experimental arrangement for the time-of-flight mass spectrometer (TOF-MS) measurements has been described previously [30]. The experimental set-up for the time-resolved (ns) surface interference fringes has been described in detail elsewhere [31]. A XeF excimer laser (Lambda Physik Lextra 200, 351 nm, 30 ns FWHM) was used as excitation source.

3. Results and discussion

The etch rates (etch depth per pulse) were calculated from linear plots of the etch depths vs. pulse number at a given fluence. All plots were linear, showing no incubation behavior as expected for highly

[1] Previously synthesized triazene-polymer (TP) had an absorption coefficient of 166 000 cm^{-1}. The difference is probably due to an incomplete diazotation and azo-coupling during the synthesis, resulting in a smaller number of triazene groups in the polymer.

absorbing polymers. Plots of the etch rates at low fluence vs. the natural logarithm of the fluence are used to calculate the ablation parameters, α_{eff} (effective absorption coefficient) and F_{th} (threshold fluence) according to Eq. (1) [32,33]:

$$d(F) = \frac{1}{\alpha_{eff}} \ln\left(\frac{F}{F_{th}}\right) \quad (1)$$

where $d(F)$ is the etch rate.

Clear differences between the etch rates of all polymers are observed in the low fluence range. This is shown in Fig. 1, where the threshold fluences and the etch rate at 100 mJ cm^{-2} are compared.

The designed polymers (MP, TM and TP) can be divided into two groups with respect to the etch rates. All triazene-containing polymers have significantly higher etch rates than the other polymers. The designed PE (MP) also reveals a higher etch rate than PI. The etch rate is independent from α_{lin} (similar for all polymers) and therefore determined by the chemical structure. For all designed polymers similar to α_{eff} of $\approx 54\,000 \pm 5000$ cm^{-1} are obtained, while PI has an α_{eff} of about 83 000 cm^{-1}. The effective absorption coefficients of the designed polymers are quite different from the linear absorption coefficient, whereas the values for PI are comparable.

The highest etch rates are obtained for TP, which has the highest triazene density per polymer chain. The same trend is also observed at high fluences, with an etch rate of up to 3 μm/pulse, and for irradiation in solution at low fluences.

All designed polymers are probably decomposing according to similar mechanisms (at least the initial steps), i.e. direct photolysis, during which homolytic bond breaking occurs [34,35]. Radicals are formed as intermediates, especially aromatic radicals, which should be present for all designed polymers. These common products/intermediates could be the reason for the very similar values of α_{eff}. In the case of polyimide different intermediates with different absorptivities are formed, i.e. quite stable amide and isocyanate intermediates were detected by FT-IR spectroscopy [36].

The designed polymers clearly reveal better ablation properties than the standard, commercial polymer (PI). All selected polymers have similar absorption

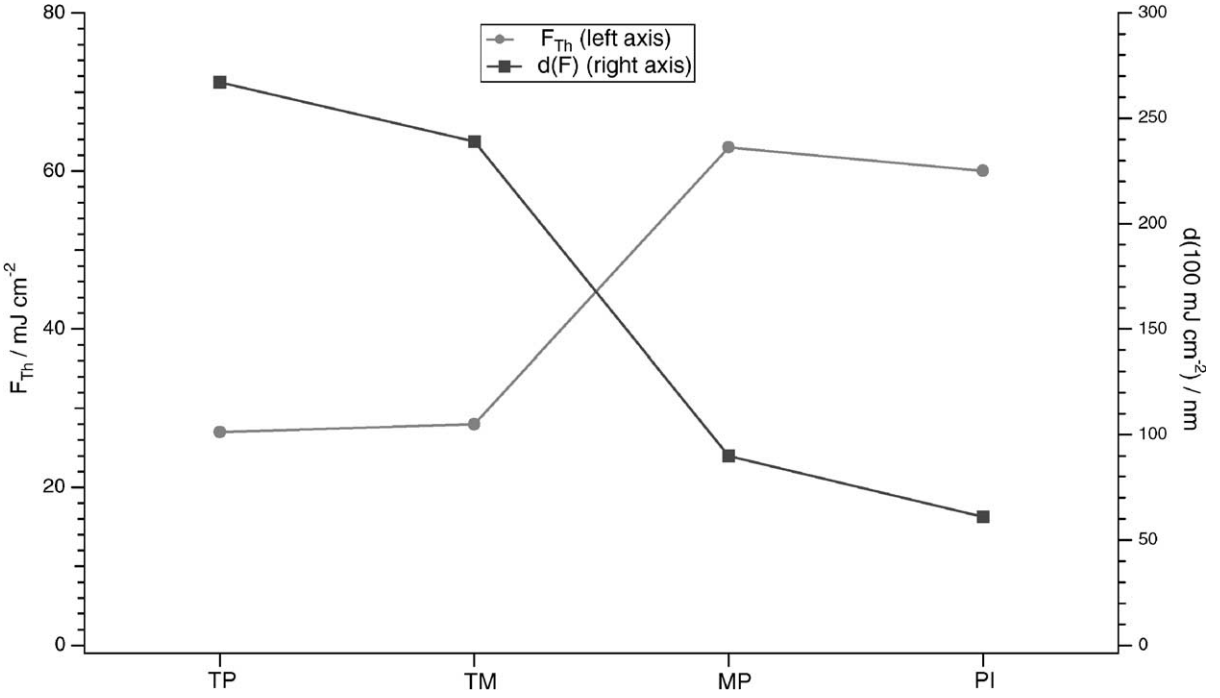

Fig. 1. Comparison of the calculated etch rates (at 100 mJ cm^{-2}) and threshold fluences for all polymers.

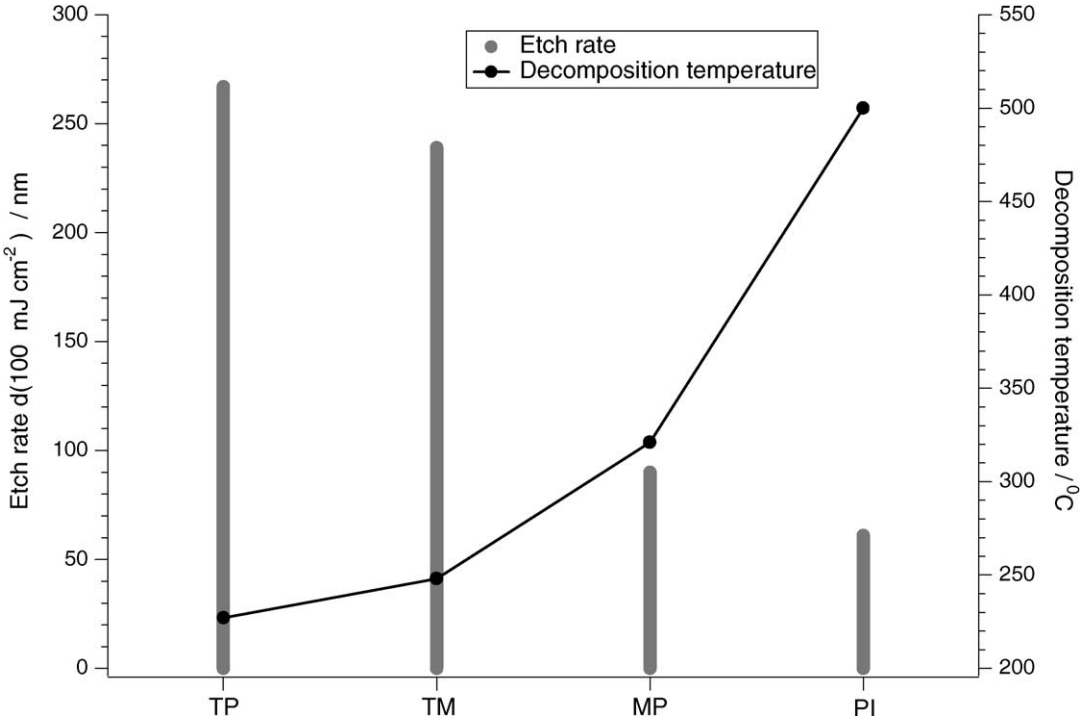

Fig. 2. Etch rates at 100 mJ cm^{-2} and decomposition temperatures of the polymers.

properties and also common structural elements (aromatic groups) ensuring that a direct comparison of the polymers is possible. The polymers containing the group (triazene) with the highest photochemical activity (TP and TM) are also the materials with the best ablation performance. This suggests that photochemical properties of specific structural units determine the ablation behavior of polymers containing these groups.

Of course one might argue that the same order of activity is also obtained if only the decomposition temperatures (T_{dec}) are considered, i.e. lowest T_{dec} for the TP- and TM-polymer, followed by MP and then PI (Fig. 2). However, a comparison reveals that the largest difference in thermal stability (170 °C) between polymers of different groups, i.e. PI and MP, corresponds to the smallest difference in ablation activity, while a much smaller difference in thermal stability (70 °C), between TM and MP, corresponds to the largest difference in ablation activity. This is even more remarkable when recalling that this is valid in a broad fluence range (from 10 to at least 400 mJ cm^{-2}), which covers a quite broad thermal range. This suggests that thermal considerations are less important for the laser ablation of these polymers. Just using the decomposition temperatures is of course a simplification, because other parameters such as thermal conductivity, specific heat, thermal diffusivity etc. are also important. The chemical structure of the polymers shows that all polymers have at least common parts in their chemical structure, suggesting that they might have comparable values for these constants, hence justifying the simplification. Photolysis experiments in solution had given the same order of photochemical activity as in the ablation experiments [26], indicating that the photochemical activity is also important for the ablation behavior. This implies also that the ablation mechanism has pronounced photochemical aspects, at least for polymers containing photochemically active groups.

A comparison of the ablation quality between a designed polymer (TP) and the standard polymer (PI) is shown in Fig. 3. The structures were created by imaging a diffractive gray tone mask onto the polymer surfaces. The experimental details are described in

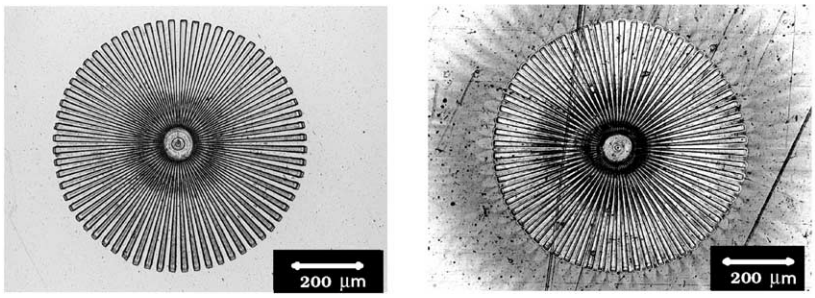

Fig. 3. SEM images of Siemens stars fabricated by laser ablation. Siemens stars in the triazene-polymer (left) and in polyimide (right) using five pulses.

detail elsewhere [37]. The structure in triazene-polymer (left) is well-defined with no debris contaminating the polymer surface, while in the case of PI pronounced contamination in the surrounding of the structure is visible. A closer inspection (not shown) reveals that contaminations are also present inside the structure and that the structure exhibits a lower resolution.

Another important aspect of ablation is the dependence of ablation parameters on the irradiation wavelength. The correlation between absorption bands, irradiation wavelengths, and ablation behavior was studied with various irradiation wavelengths, i.e. 193, 266, 308 and 351 nm. In Fig. 4 the etch rates observed with TP for the different irradiation wavelengths are

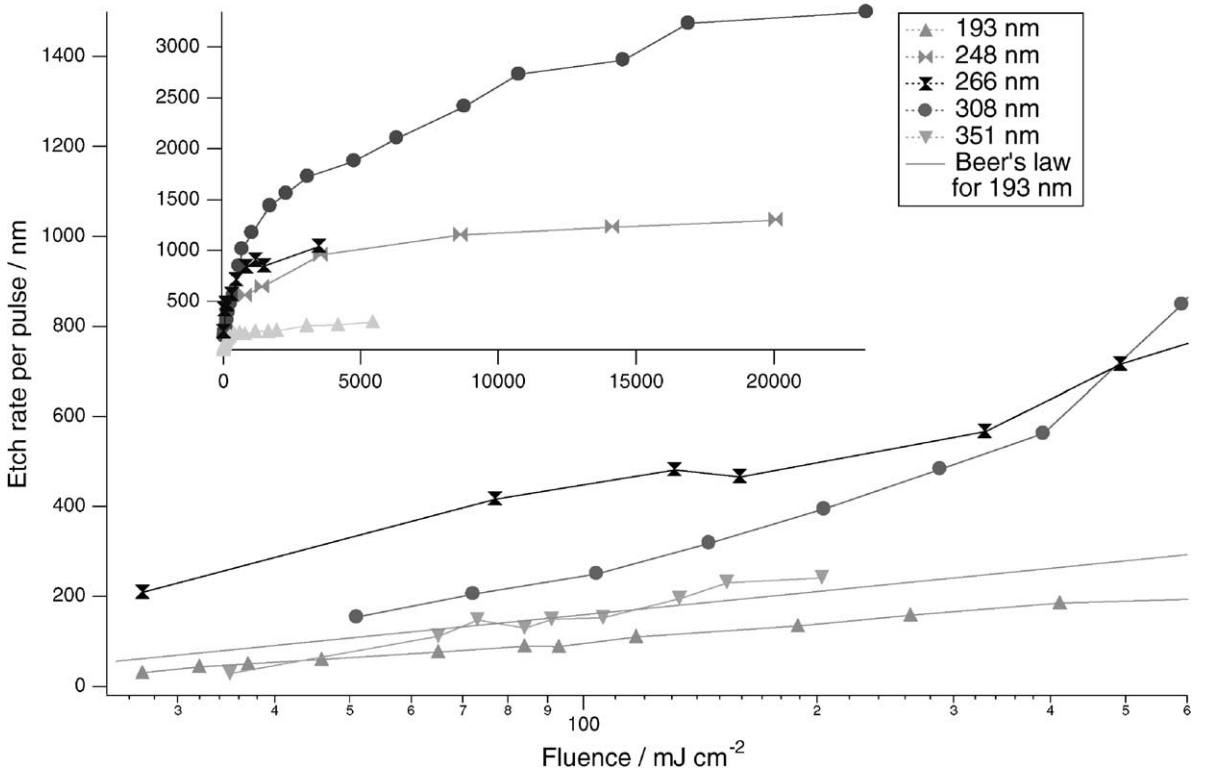

Fig. 4. Measured etch rates of TP vs. the logarithm of the fluence (up to 600 mJ cm^{-2}) for different irradiation wavelengths. Inset shows the same plot for the complete linear fluence range.

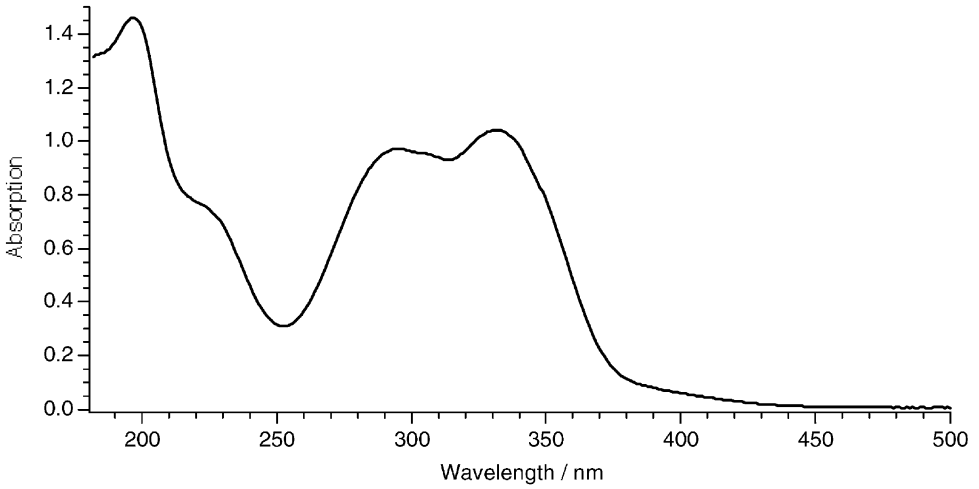

Fig. 5. UV–Vis absorption spectra of the TP-polymers. Thin film coated from chlorobenzene onto a quartz wafer.

shown for low fluences on a logarithmic scale and on a linear scale for the complete fluence range (inset in Fig. 4). In the high fluence range data points for 248 nm irradiation from a previous study [14] are included. The data points seem to fit quite well to the 266 nm irradiation data. The different irradiation wavelengths correspond to different features of the UV–Vis spectrum (Fig. 5). The spectrum reveals two strong bands around 196 nm, corresponding mainly to the aromatic parts of the polymer, and 332 nm, corresponding mainly to the triazene chromophore [38]. The etch rates can more or less be divided into two groups (shown in Fig. 4), i.e. the wavelengths which directly excite the triazene system (266, 308 and may be 351 nm) and 193 nm that is in resonance with the aromatic system. Irradiation with 193 nm results in the lowest ablation rates, which are even below the etch rates described in Eq. (1) using the linear absorption coefficient α_{lin} from Beer's law (included in Fig. 4). This is very different to the other irradiation wavelengths, where much higher etch rates result than predicted by Beer's law. This is most probably due to decomposition (ablation, see below) of the polymer during the pulse. The difference between 308 and 193 nm is even more remarkable when we consider that the absorption coefficients are quite similar. The etch rates of the three wavelengths which are in resonance with the triazene chromophore follow, at low fluences, the values of photon energy (highest photon energy = highest etch rate). At higher fluences lower etch rates are obtained for 266 nm as compared to 308 nm irradiation (see inset Fig. 4). This can be explained by absorption of the laser photons by the ablation products in the gas phase (shielding), especially by aromatic radicals. It is also noteworthy that the etch rates obtained for 193 and 266 nm irradiation follow a linear relation (on the logarithmic fluence-scale) over the whole fluence range. For all irradiation wavelengths similar low threshold fluences result, i.e. 12 ± 2 mJ cm^{-2} for 193 nm, 8 ± 2 mJ cm^{-2} for 266 nm, 27 ± 3 mJ cm^{-2} for 308 nm, and 25 ± 3 mJ cm^{-2} for 351 nm irradiation. This suggests that with all irradiation wavelengths the same reactions are induced. This is most probably the decomposition of triazene system, where homolytic bond breakage of the N–N single bond can be achieved with the energy of a single photon at all irradiation wavelengths.

3.1. TOF-MS

For a better understanding of the ablation mechanisms of the designed photopolymers, one polymer was selected (TP) and studied in more detail. An additional feature of this polymer is visible in the UV–Vis spectrum (Fig. 5). The absorption maximum is close to the irradiation wavelength of 308 nm, while an absorption minimum is at another excimer laser

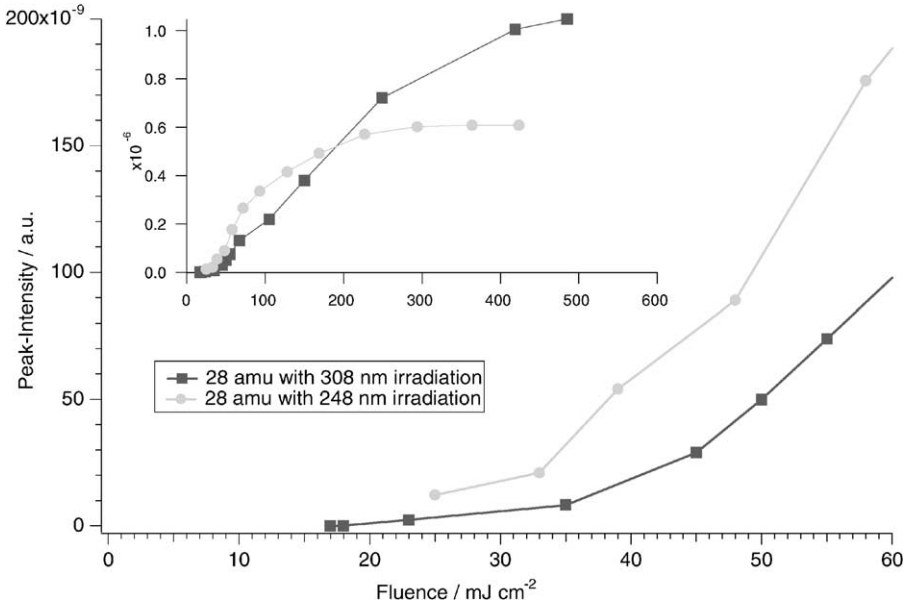

Fig. 6. Intensity of the 28 amu signal from decomposition of TP at various fluences with 248 and 308 nm irradiation.

emission wavelength, i.e. 248 nm. A comparison of these two irradiation wavelengths could give valuable information about the influence of these structural units on the ablation mechanism. As analytical method TOF-MS was selected, because different products of ablation, or intensities of products, can give a direct indication for a different ablation mechanism. Previous studies [39,40] with 248 nm and detailed analysis of the time-of-flight curves had shown that fragment emission follows an Arrhenius relation, where the temperature is predicted from the total deposited laser energy. For a direct comparison between the two irradiation wavelengths, the relative maximum peak intensities of different fragments are compared. In Fig. 6 the response of the most intense mass (i.e. 28 amu from N_2) at the two different irradiation wavelengths is compared. The data taken after irradiation at 308 nm exhibit a linear increase of the signal intensities at low fluences (<40 mJ cm^{-2}). At higher fluences a fast increase is observed, as shown in the inset in Fig. 6. This is an indication that at fluences above ≈40 mJ cm^{-2}, the process changes from a linear photochemical reaction to the non-linear ablation process. This value agrees very well with the ablation threshold of ≈25–30 mJ cm^{-2}, which was determined with other techniques [38,41]. Upon irradiation at 248 nm a much faster increase of the signal was detected and no linear range can be observed (Fig. 6). At higher fluences the signal intensity reaches a maximum (inset in Fig. 6). All other detected fragments, which can be assigned directly to ablation, reveal lower intensities (with constant values at higher fluences) for 248 nm irradiation. This is probably due to absorption of the incoming photons by the fragments (e.g. aromatic radicals, which are produced during ablation) and the decomposition of the absorbing fragments in the gas phase.

3.2. Excimer-lamp irradiation

Excimer-lamps were applied to study the low fluence irradiation region, where linear photochemistry (no ablation) is taking place. This is in the fluence range (Fig. 6), where a linear relation between reaction products and laser fluence is observed. The excimer-lamps emit at the same wavelength as the excimer laser, but with incoherent radiation, and in quasi-CW mode. The peak photon fluxes of the lamps are also low compared to the excimer laser, suggesting that multi-photon processes are not important (irradiance ≈25 mW cm^{-2}). Thin films of the TP-polymer on quartz substrates were irradiated with the excimer-lamps. As irradiation

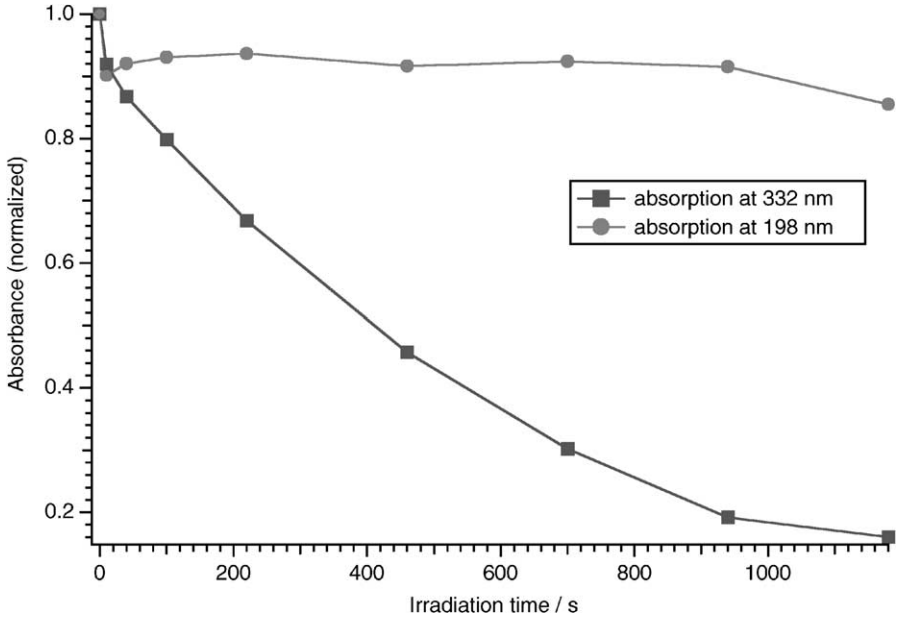

Fig. 7. Change of the absorption at 332 and 198 nm at various irradiation times with 308 nm. The irradiation was performed in air and the absorption was normalized to 1.

source a XeCl (308 nm), a KrCl (222 nm) and a Xe_2 (172 nm) excimer-lamps were selected. Excimer-lamps based on fluorine containing excimers are difficult to operate, due to etching of the quartz housing by the F_2. Therefore the KrCl excimer-lamp was used instead of the KrF (248 nm) irradiation, and additionally the Xe_2 excimer-lamp. The thin polymer films were irradiated for certain time periods, followed by analysis with the UV–Vis spectrometer. The decomposition of the polymer was analyzed at the two maxima, i.e. 198 and 332 nm. With 308 nm irradiation nearly exclusively decomposition of the triazene group (332 nm) can be observed with only very minor changes for the 198 nm band (shown in Fig. 7). In the case of 222 and 172 nm irradiation both bands are decreasing (not shown).

The excimer-lamp irradiation experiments show clearly that photochemical decomposition of the TP-polymer takes place, even at low fluences and quasi-CW irradiation (the excimer-lamps emit burst of UV pulses with nanosecond duration, but with repetition frequencies in the kHz range). With 308 nm irradiation only the triazene group decomposes, while for all other irradiation wavelengths all bands in the UV spectra decrease.

3.3. Nanosecond-Interferometry

The UV–Vis (after excimer-lamp irradiation) and TOF-MS experiments strongly indicate that photochemical reactions are important in the low fluence range (below and just above the threshold of ablation). Another technique that can give indications about the ablation mechanism is nanosecond-interferometry. It has been shown in previous studies [42,43] that thermal/photothermal ablation results first in pronounced swelling of the polymer surface, followed by etching. The etching takes place on times scales much longer than the pulse length of the excimer laser (up to the micro-second range). TP and PI were studied with an irradiation wavelength of 351 nm. The ablation threshold for TP at 351 nm is $\approx$25 mJ cm^{-2}, while PI exhibits a threshold of 210 mJ cm^{-2}. The experiments were performed with fluences above the threshold of ablation, i.e., 223 mJ cm^{-2} for TP and 460 mJ cm^{-2} for PI. The results are shown in Fig. 8. The etching of the triazene-polymer starts and ends within the excitation pulse of the excimer laser. Prior to etching, darkening of the surface is observed, which is probably due to the creation of the first products, i.e., N_2, inside the polymer [44]. The overestimation of the

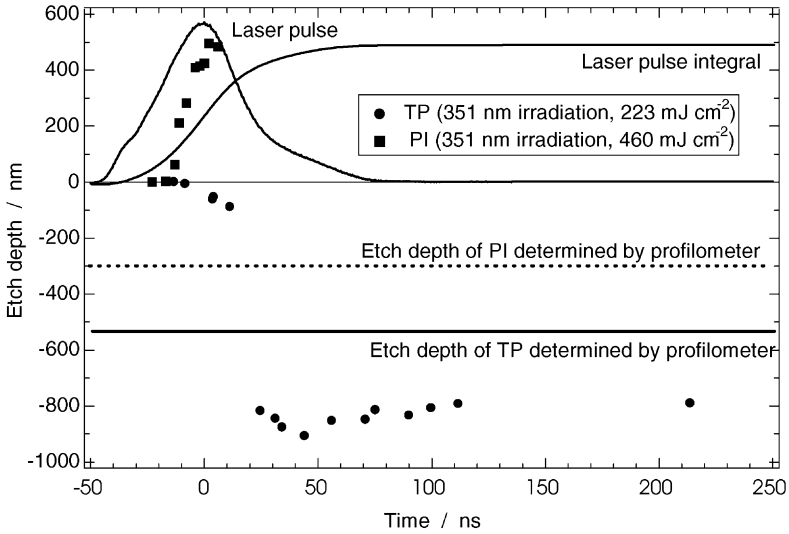

Fig. 8. Nanosecond expansion/etching behavior of the triazene-polymer and polyimide after 351 nm irradiation.

etch depths is due to the experimental configuration, described in detail elsewhere [44]. In the case of PI a very different behavior is observed. It was only possible to observe swelling of the polymer surface (up to several hundred nanometer) up to several nanosecond. At longer time scales the surface could not be observed, probably due to the ejection of large solid fragments which shield the probe light.

The differences between TP and PI in the dynamic interferometric studies suggest again that different mechanisms are active for TP and PI. We have strong indication for a partly photochemical ablation mechanism for TP, i.e., products of decomposition at low fluences, sharp threshold and clean etching within the time scale of the laser pulse. In the case of PI a photothermal mechanism is more probable, e.g., swelling and etching on time scales longer than the laser pulse.

4. Conclusions

The ablation characteristics of various polymers were studied at low and high fluences. The polymers can be divided into three groups, i.e. polymers containing triazene and ester groups, the same polymers without the triazene group, and polyimide as reference polymer. At high fluences similar ablation parameters, i.e. etch rates and effective absorption coefficients, were obtained for all polymers. The main difference is the absence of carbon deposits for the designed polymers. At low fluences (at 308 nm) very pronounced differences are detected. The polymers containing the photochemically most active group (triazene) exhibit the lowest threshold of ablation (as low as 25 mJ cm^{-2} for 308 nm) and the highest etch rates (up to 3 μm/pulse), followed by the designed PEs and then polyimide. Other irradiation wavelengths reveal also very low threshold fluences (between 8 and 25 mJ cm^{-2}), but also pronounced differences in the etch rates. Irradiation at wavelengths (266, 308 and 351 nm) which are in resonance with the absorption band of the triazene chromophore results in much higher etch rates than irradiation at a shorter wavelength (193 nm) which is in resonance with the aromatic system of the polymer. The laser-induced decomposition of a designed polymer and polyimide were studied by nanosecond-interferometry with 351 nm irradiation. Only the triazene-polymer reveals etching without any sign of surface swelling, which is observed for polyimide. The etching of the triazene-polymer starts and ends with the laser pulse, clearly indicating photochemical etching.

The intensities of the ablation fragments analyzed by TOF-MS show pronounced differences between irradiation at the absorption band of the triazene group (308 nm) and irradiation at a shorter wavelength (248 nm). The larger fragments reveal lower intensities

for 248 nm irradiation, due to the additional decomposition of these fragments by the higher energy of 248 nm photons and the lower etch rates for 248 nm irradiation. With 308 nm irradiation the intensity of the main fragment (N_2) increases linearly with fluences that are probably below the threshold of ablation, suggesting that photochemical decomposition take place. This was confirmed by excimer-lamp irradiation, which also revealed a decomposition of the triazene group at fluences well below the threshold of ablation.

Acknowledgements

This work has been supported be the Swiss National Science Foundation and a NATO Grant for International Collaboration (CRG 973063).

References

[1] A.L. Schawlow, Science 149 (1965) 13.
[2] L. Longo (Ed.), A Window on the Laser Medicine World, SPIE2000, Bellingham, Washington, 2000.
[3] V. Zafiropulos, C. Fotakis, in: M. Cooper (Ed.), Laser Cleaning in Conservation, Butterworth Heinemann, Oxford, 1998, p. 79.
[4] D.B. Chrisey, G.K. Hubler (Eds.), Pulsed Laser Deposition of Thin Films, Wiley, New York, 1994.
[5] R. Srinivasan, V. Mayne-Banton, Appl. Phys. Lett. 41 (1982) 576.
[6] Y. Kawamura, K. Toyoda, S. Namba, Appl. Phys. Lett. 40 (1982) 374.
[7] K. Suzuki, M. Matsuda, T. Ogino, N. Hayashi, T. Terabayashi, K. Amemiya, Proc. SPIE 2992 (1997) 98.
[8] F. Raimondi, S. Abolhassani, R. Brütsch, F. Geiger, T. Lippert, J. Wambach, J. Wei, A. Wokaun, J. Appl. Phys. 88 (2000) 1.
[9] R. Srinivasan, B. Braren, R. Dreyfus, J. Appl. Phys. 56 (1987) 372.
[10] S. Lazare, V. Granier, Laser Chem. 10 (1989) 25.
[11] R. Srinivasan, B. Braren, Chem. Rev. 89 (1989) 1303.
[12] P.E. Dyer, in: I.W. Boyd, R.B. Jackman (Eds.), Photochemical Processing of Materials, Academic Press, London, 1992, p. 359.
[13] N. Arnold, N. Bityurin, Appl. Phys. A 68 (1999) 615.
[14] T. Lippert, J. Stebani, J. Ihlemann, O. Nuyken, A. Wokaun, Angew. Makromol. Chem. 206 (1993) 97.
[15] T. Lippert, J. Stebani, J. Ihlemann, O. Nuyken, A. Wokaun, J. Phys. Chem. 97 (1993) 12296.
[16] T. Lippert, Th. Kunz, C. Hahn, A. Wokaun, Recent Res. Dev. Macromol. Res. 2 (1997) 121.
[17] O. Nuyken, U. Dahn, N. Hoogen, D. Marquis, M.N. Nobis, C. Scherer, J. Stebani, A. Wokaun, C. Hahn, Th. Kunz, T. Lippert, Polym. News 24 (1999) 257.
[18] O. Nuyken, C. Scherer, A. Baindl, A.R. Brenner, U. Dahn, R. Gärtner, S. Kaiser-Röhrich, R. Kollefrath, P. Matusche, B. Voit, Prog. Polym. Sci. 22 (1997) 93.
[19] L.S. Bennett, T. Lippert, H. Furutani, H. Fukumura, H. Masuhara, Appl. Phys. A 63 (1996) 327.
[20] T. Lippert, S.C. Langford, A. Wokaun, S. Georgiou, J.T. Dickinson, J. Appl. Phys. 86 (1999) 7116.
[21] T. Lippert, T. Nakamura, H. Niino, A. Yabe, Macromolecules 29 (1996) 6301.
[22] T. Lippert, J. Wei, A. Wokaun, N. Hoogen, O. Nuyken, Appl. Surf. Sci. 168 (2000) 270.
[23] Th. Kunz, J. Stebani, J. Ihlemann, A. Wokaun, Appl. Phys. A 67 (1998) 347.
[24] O. Nuyken, J. Stebani, T. Lippert, A. Wokaun, A. Stasko, Macromol. Chem. Phys. 196 (1995) 739.
[25] N. Hoogen, O. Nuyken, J. Polym. Sci. Polym. Chem. 38 (2000) 1903.
[26] J. Wei, N. Hoogen, T. Lippert, O. Nuyken, A. Wokaun, J. Phys. Chem. B 105 (2001) 1267.
[27] B. Eliasson, U. Kogelschatz, Appl. Phys. B 46 (1988) 299.
[28] U. Kogelschatz, Pure Appl. Chem. 62 (1990) 1667.
[29] J.-Y. Zhang, H. Esrom, I.W. Boyd, Appl. Surf. Sci. 138–139 (1999) 315.
[30] J.J. Shin, D.R. Ermer, S.C. Langford, J.T. Dickinson, Appl. Phys. A 64 (1997) 7.
[31] H. Furutani, H. Fukumura, H. Masuhara, Appl. Phys. Lett. 65 (1994) 3413.
[32] J.E. Andrews, P.E. Dyer, D. Forster, P.H. Key, Appl. Phys. Lett. 43 (1983) 717.
[33] R. Srinivasan, B. Braren, J. Polym. Sci. 22 (1984) 2601.
[34] T. Lippert, J. Stebani, O. Nuyken, A. Stasko, A. Wokaun, J. Photochem. Photobiol. A 78 (1994) 139.
[35] A. Stasko, V. Adamcik, T. Lippert, A. Wokaun, J. Dauth, O. Nuyken, Makromol. Chem. 194 (1993) 3385.
[36] E.E. Ortelli, F. Geiger, T. Lippert, J. Wei, A. Wokaun, Macromolecules 33 (2000) 5090.
[37] C. David, J. Wei, T. Lippert, A. Wokaun, Microlectr. Eng. 57–58 (2001) 453.
[38] T. Lippert, L.S. Bennett, T. Nakamura, H. Niino, A. Ouchi, A. Yabe, Appl. Phys. A 63 (1996) 257.
[39] T. Lippert, A. Wokaun, S.C. Langford, J.T. Dickinson, Appl. Phys. A 69 (1999) S655.
[40] T. Lippert, S.C. Langford, A. Wokaun, S. Georgiou, J.T. Dickinson, J. Appl. Phys. 86 (1999) 7116.
[41] T. Lippert, L.S. Bennett, T. Nakamura, H. Niino, A. Yabe, Appl. Surf. Sci. 96–98 (1996) 601.
[42] H. Furutani, H. Fukumura, H. Masuhara, J. Phys. Chem. 100 (1996) 6871.
[43] H. Furutani, H. Fukumura, H. Masuhara, S. Kambara, T. Kitaguchi, H. Tsukada, T. Ozawa, J. Phys. Chem. B 102 (1998) 3395.
[44] H. Furutani, H. Fukumura, H. Masuhara, T. Lippert, A. Yabe, Phys. Chem. A 101 (1997) 5742.